Digital beacon receiver for ionospheric TEC measurement developed with GNU Radio

Mamoru Yamamoto

Research Institute for Sustainable Humanosphere, Kyoto University, Gokasho, Uji, Kyoto 611-0011, Japan

A simple digital receiver named "GNU Radio Beacon Receiver (GRBR)" was developed for the satellite-ground beacon experiment to measure the ionospheric total electron content (TEC). The open-source software toolkit for the software defined radio, GNU Radio, is utilized to realize the basic function of the receiver and perform fast signal processing. The software is written in Python for a LINUX PC. The open-source hardware called Universal Software Radio Peripheral (USRP), which best matches the GNU Radio, is used as a front-end to acquire the satellite beacon signals of 150 and 400 MHz. The first experiment was successful as results from GRBR showed very good agreement to those from the co-located analog beacon receiver. Detailed design information and software codes are open at the URL http://www.rish.kyoto-u.ac.jp/digitalbeacon/.
Key words: Satellite-ground beacon experiment, software-defined radio, ionospheric total electron content.

1. Introduction

The ground-based reception of radio beacon signals transmitted from Low Earth Orbit Satellites (LEOS) is a historical method to measure the total electron content (TEC) of the ionosphere. Observations of this kind were initiated right from the beginning of the space era (e.g., Aitchison and Weekes, 1959; Garriott, 1960). The principle of the experiment is based on the frequency dependence of the refractive index of radio waves in the ionospheric plasma. The most commonly used frequencies are 150 and 400 MHz—in a ratio of 3:8—generated from a common oscillator signal at 50 MHz. The most common beacon satellite constellation is the polar-orbiting Navy Navigation Satellite System (NNSS) (Leitinger *et al.*, 1984). One of the recent developments of the TEC measurement is the use of GPS receivers. We now have both world-wide and regional networks of GPS receivers that constantly monitor large-scale structures of the ionosphere (e.g., Saito *et al.*, 1998). The LEOS beacon experiment should be complimentary to these by providing information on the smaller scale structures. Another improvement is the use of a third frequency to enhance the robustness of the experiment (Bernhardt and Siefring, 2006). Such tri-band beacon transmitters are now on board several LEOS, such as, in the FORMOSAT-3/COSMIC constellation (Lion *et al.*, 2007) and C/NOFS (De La Beaujardière *et al.*, 2004).

Beacon receivers developed in the past have been mostly analog receivers for 150- and 400-MHz signals, and some of these are commercially available. The phase relationship between the two signals is detected by an analog circuit, and the resultant phase values are digitized at several tens of Hertz only. One digital receiver was devel-

oped as a special piece of equipment on board the CITRIS satellite (Bernhardt and Siefring, 2006). The development of a software-defined radio (SDR) system is now possible by using off-the-shelf universal hardware and software for digital signal processing. A digital receiver for the dual-band LEOS beacon reception has been developed based on the open-source software toolkit named GNU Radio (http://gnuradio.org/) and its friendly open-source hardware called Universal Software Radio Peripheral (USRP) (http://www.ettus.com/). The aim of this paper is to describe the hardware and software of the new beacon receiver and to show an example of its successful TEC measurement.

2. Basic Description of the Dual Beacon Experiment

The theoretical framework of the beacon TEC measurements is discussed, for example, by Davies (1980) and references therein. Radio wave propagation in a plasma with refractive index n is expressed as

$$u = U \cos\left\{2\pi f\left(\frac{x}{c_\mathrm{p}} - t\right)\right\} = U \cos\left\{2\pi f\left(\frac{nx}{c} - t\right)\right\} \quad (1)$$

where U is amplitude, f is frequency, c_p is phase velocity, $c = 2.998 \times 10^8$ m s^{-1} is the speed of light, x is position, and t is time. The refractive index n at VHF or higher frequencies can be simply described by a function of f [Hz] and number density of free electrons in plasma N [m^{-3}] as

$$n = c/c_\mathrm{p} = 1 - \left\{A \big/ \left(2f^2\right)\right\} N \quad (2)$$

where, $A = \frac{e^2}{(2\pi)^2 m\epsilon_0} = 80.6$ m^3 s^{-2}, $\epsilon_0 = 8.854 \times 10^{-12}$ F m^{-1} is the permittivity of free space, and $e = -1.602 \times 10^{-19}$ C and $m = 9.109 \times 10^{-31}$ kg are the charge and mass of an electron, respectively. Total phase Ψ at travel length L is described as

$$\Psi = \frac{2\pi f}{c}L - \frac{\pi A}{cf}\int N\mathrm{d}x + \eta \quad (3)$$

where $\int N \mathrm{d}x$ is TEC, and η is the system phase bias that is an unknown constant. We can eliminate L by using two radio waves at $f_1 = pf_{\mathrm{r}}$ and $f_2 = qf_{\mathrm{r}}$. Normally, we use $f_{\mathrm{r}} = 50$ MHz, $p = 3$, and $q = 8$, i.e., $f_1 = 150$ MHz and $f_2 = 400$ MHz. The phases corresponding to both frequencies are Ψ_1 and, Ψ_2, and the phase difference Φ at f_{r} is written as follows.

$$\Phi = \frac{\Psi_1}{p} - \frac{\Psi_2}{q} = \frac{\pi A}{f_{\mathrm{r}} c} \left(\frac{1}{q^2} - \frac{1}{p^2} \right) \int N \mathrm{d}x + \eta' \quad (4)$$

In this technique, TEC is measured as the difference of path length of signals at two frequencies. As Eq. (4) is its expression in phase, there is an inherent ambiguity that actually comes as integer multiples of 2π. Also, the system phase bias remains as described by η'. According to the motion of the satellite, TEC between the satellite and the receiver, which is the slant TEC, varies in time. This is due to the change in the elevation angle of the satellite and is also caused by the spatial variation of the ionospheric plasma. The ground-based receiver then measures the relative variation of the slant TEC during the satellite pass. Absolute TEC can be estimated, for example, if we have data from two or more locations (Leitinger *et al.*, 1975). This is, however, beyond the scope of this short paper.

In conventional analog receivers, the calculations of Ψ_1/p and Ψ_2/q in Eq. (4) are realized by the phase-locked loop (PLL) circuitry. In our digital receiver system, on the other hand, the phase of both signals are separately evaluated by digital processing, and TEC is calculated as described in Section 4.

3. System Description of the Receiver

GNU Radio is an excellent software toolkit for implementing the SDR systems. Its front-end is based on the script language Python, while the performance-critical engine of the digital signal processing is written in C++. Because of this software design, developers can select functions suitable for their specific requirements from Python codes, define the flow of signal processing, and run the program. The programing style is analogous to the design of hardware radio, i.e., determine the functions of the system, organize them as a block diagram, then implement the radio. It is also possible to expand the capabilities of the GNU Radio by adding more signal processing codes in C++. The advantage of the GNU Radio is enhanced by its friendly hardware for data acquisition, called the USRP. The USRP consists of a main board connected to a host computer through the USB 2.0 interface. It can be operated as a two-channel receiver and a two-channel transmitter simultaneously. In the receiving mode, the USRP main board has four analog-to-digital converters (ADC), each with 12 bits per sample, 64 M sample/s; it is sensitive to signal frequencies of about 200 MHz. All analog signals are fed through daughter boards that can be attached to the main board, and some daughter boards can down-convert the signal frequency by analog circuitry. An FPGA (field-programmable gate array) on the USRP main board is used for fast digital processing. By selecting specific daughter boards, the USRP is applicable to various radio systems in the frequency range from near DC to several GHz. The GNU Radio and USRP are both an open-source software
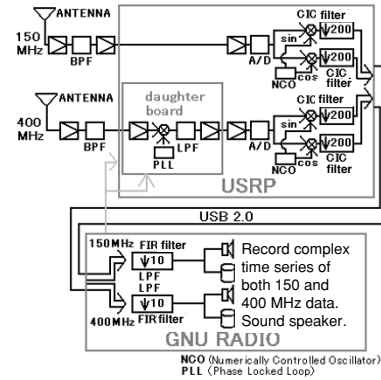

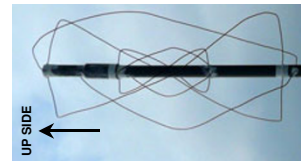Fig. 1. Block diagram of the GNU Radio Beacon Receiver (GRBR).

Fig. 2. Quadrifilar helix (QFH) antenna for the 150- and 400-MHz beacon. (Note: Tilted $90°$ to the left for editorial reason.)

and hardware, respectively, so that all information, including circuit design and FPGA code, is open.

Figure 1 shows the block diagram of the newly developed receiver. A LINUX PC and the USRP are the main components. Signals from 150- and 400-MHz antennas are amplified and filtered by band-pass filters (BPFs) for anti-aliasing purpose. The 150-MHz signal is directly applied to the ADC, and the undersampled digital signal is aliased into 22 MHz. The 400-MHz signal is down converted to less than 10 MHz on the daughter board and then sampled by the ADC at the same rate. Further signal processing is carried out in the FPGA on the main board, as follows. The digitized signals are multiplied with 'SIN' and 'COS' signals generated by the NCO (numerically controlled oscillator), and converted to the base-band complex signals. The total effective sampling speed is then reduced to 320 kHz, corresponding to a decimation factor of 200, after low-pass filtering by the CIC (cascaded integrator-comb) filter. After transferring the data to the LINUX PC, the GNU Radio program further limits the signal bandwidth by a FIR (finite impulse-response) filter and reduces the sample rate to 32 kHz. The expected Doppler shift at 400 MHz is about ± 10 kHz, which is well within the final bandwidth. Both signals are then stored in separated files as discrete series of complex data. Sound monitoring of the signals is also possible.

The QFH (quadrifilar helix) antenna is an unique antenna that has a quasi omni-directional beam pattern of the circular-polarized radio wave and is suitable for the LEOS beacon experiment (e.g., Kilgus, 1969; Adams *et al.*, 1974). The QFH antennas were in-house fabricated with PVC pipes and copper wires, as shown in Fig. 2. The 400-MHz antenna element is nested inside the 150-MHz element to avoid phase variation owing to the satellite motion. The intensity of the beacon signals is estimated by assuming the transmission of 1 W from a LEOS, the maximum propagation distance of 4000 km, and the use of

omni-directional antennas at both ends. Power and voltage into a 50-Ω load induced at the receiving antenna are 1.6×10^{-15} W and 2.8×10^{-7} V at 150 MHz, and 2.3×10^{-16} W and 1.1×10^{-7} V at 400 MHz, respectively. The smallest detectable voltage of the ADC is about 0.5 mV, considering its 12-bit resolution to the ±1 V input. Hence, the necessary amplification from antenna to the ADC is then 65 dB and 74 dB for 150 and 400 MHz, respectively. For this system, pre-amplifiers are located at the bottom of the antennas. An additional amplifier is used for the 150 MHz signal. The daughter board for 400 MHz has enough amplification on its own.

With reference to the hardware design, it should be noted that selection of the anti-aliasing filters is important to avoid unexpected radio interference. It is also important to set the gain of the amplifiers so as to avoid signal saturation. Saturation of any signal, even if it occurs at a different frequency range, can cause significant signal distortion. As the frequency of the NCO is discretely selected, residual frequency on the order of mHz may remain in the USRP tuning. This very small offset that breaks the 3:8 frequency ratio can result in an detectable constant increase or decrease of the measured TEC. Careful selection of the tuning frequency reduces the problem. Nevertheless, based on these tests with accurate signal sources, it is confirmed that a compensation in the analysis is also possible.

4. Analysis for TEC Estimation

Estimation of TEC from the digital receiver is conducted by off-line data analysis. The process can be categorized as follows; (1) spectral peak finding, (2) narrow filtering of beacon signal, and (3) phase detection and TEC estimation.

(1) The raw data are stored as time series of 32-kHz sampled complex numbers that consist of both signal and noise. We first calculate the power spectrum of the data by 8192-point FFT. The Nyquist limit of the spectrum is ±16 kHz, and the distance between spectral points is 3.91 Hz, corresponding to 0.256-s long data. The beacon signal appears as an intense peak in each spectrum with the Doppler frequency shift corresponding to the satellite motion relative to the receiver. With the help of a priori information on the satellite motion, an attempt is made to find the best candidate peak of the signal from both 400- and 150-MHz spectra. The precise intensity and frequency of the signals are then estimated by the zeroth and first order moments of several spectral components around the peak, respectively.

(2) The "beacon only" signals are extracted by using "FFT band-pass filtering". We select three (for 150 MHz) and seven (for 400 MHz) complex components of the spectrum around the peak frequency, fill zero to all other components, and calculate complex time series by the inverse FFT. This is a very narrow BPF with a pass-band width of only 20–30 Hz. In order to avoid Gibb's effect of the filtered results, we use only the center half portion of the results and then stagger the calculation by half of the FFT points.

(3) The phase difference between two filtered signals is evaluated at the common frequency. Assuming that the filtered results are a pure sinusoidal complex time series, "M-th power" of the data is to multiply the signal frequency by the factor M. We then calculate $s_i = (x_i)^8 / (y_i)^3$, where x_i and y_i denote discrete complex time series with the index

i at 150 and 400 MHz, respectively. The phase angle of s_i is the differential phase Φ' evaluated at the frequency of the least common multiple of two frequencies, $pq f_r$. The equation for Φ' is

$$\Phi' = pq\Phi = \frac{\pi A}{f_r c}\left(\frac{p}{q} - \frac{q}{p}\right)\int N\,\mathrm{d}x + pq\eta' \quad (5)$$

Note that this expression is different from Φ of Eq. (4) in which the common frequency was selected as the greatest common divisor, f_r. As Φ' causes number of 2π phase wrapping in time, the phase values are carefully unwrapped throughout the observation period and the relative variation of slant TEC is obtained during the satellite pass.

5. Results from the First Observation

The first observations with the new digital beacon receiver were conducted in August–September 2007 in the Uchinoura Space Center of JAXA (Japan Aerospace Exploration Agency) (31.3°N, 131.1°E). At the same location we fortunately had an analog beacon receiver, the Coherent Ionosphere Doppler Receiver (CIDR) developed at the University of Texas at Austin (Coker *et al.*, 2004). Figure 3 shows the digital-receiver record of intensity and frequency of signals from the FORMOSAT-3/COSMIC satellite constellation. The pass was on August 31, 2007 at 15:35–15:51 UT, which is close to local midnight (the local standard time is UT +9 h). The satellite FM5 of the FORMOSAT-3/COSMIC constellation appeared from the south horizon at azimuth 193°, reached the maximum elevation 77° at 15:43 UT, and set in the north horizon at azimuth 21°. The intensity includes signal and noise power, and the unit is relative. The signal was lost after 890 s, and the intensity dropped down to the noise level. From this figure we can see that the maximum signal-to-noise ratio for 150 and 400 MHz is more than 40 and 30 dB, respectively. There were several drop-offs of the signal, and some of these suffered mis-estimation of the frequency. The signals show overall negative frequency offset, which is due to frequency offset of the time base on the USRP main board. This is a hardware limitation of using a small crystal oscillator (64 MHz) without temperature control. However, this does not affect the results because the TEC estimation de-
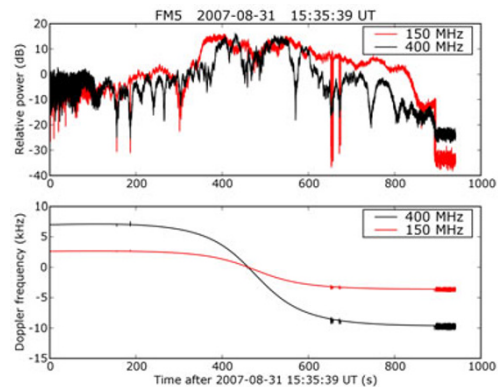

Fig. 3. Signal strength (top) and Doppler frequency (bottom) of the signal from FORMOSAT-3/COSMIC FM5 on August 31, 2007 at 15:35:39 UT. Data of 400- and 150-MHz signals are shown by black and red lines, respectively.
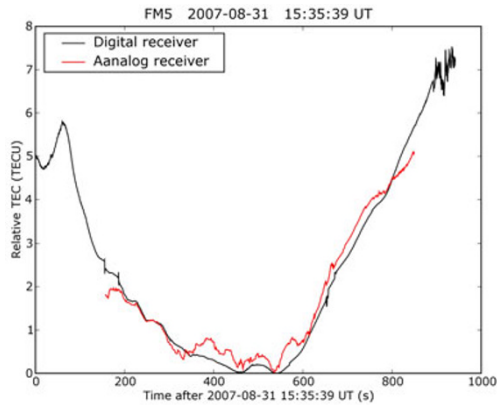
Fig. 4.   Relative TEC estimated by the digital receiver (black line) and co-located analog receiver CIDR (red line) from FORMOSAT-3/COSMIC FM5 on August 31, 2007 at 15:35:39 UT.

pends on the phase coherency between the two frequencies that is strictly maintained over the USRP main board and the daughter board.

Estimated TEC from the digital and analog receivers are shown by black and red lines in Fig. 4, respectively. Both are the relative slant TEC, as described in Section 2. Data are then plotted by shifting each minimum to zero. The ordinate is in the TEC unit defined as $1\,\mathrm{TECU} = 10^{16}$ electrons/m^2.

The TEC from the digital receiver is averaged over 0.128 s and plotted at the same interval. The result from the analog receiver is plotted at each second. The digital receiver could estimate TEC in the time range of 70–890 s, corresponding to the satellite elevation $>5°$. This is much better than the CIDR because of careful off-line data analysis in the digital receiver. The discrepancy between both TEC is typically 0.2 TECU or less and did not exceed 0.5 TECU throughout the experiment. Both slant TEC records show parabolic variation owing to the time-varying elevation of the satellite. Small-scale perturbations are similarly seen in both datasets, and the amplitude and phase well match each other. It is possible that these variations are due to the medium-scale traveling ionospheric disturbance (MSTID) that is frequently seen in summer nighttime over Japan (Saito et al., 1998). Simultaneous GPS-TEC data from GEONET show weak patterns of MSTID near the observation region with an amplitude of about ±0.2 TECU. Several sudden jumps of TEC are also seen at 155, 185, 570 s and 650–675 s, which correspond to drop-offs of signal intensity. Some of these are also seen in the CIDR data. These glitches, however, can be removed in subsequent data analysis. There is a tendency that TEC from the digital receiver is smoother than those from the CIDR. A detailed comparison of the accuracies will be discussed in a future paper. These results clearly show that TEC measurement by the digital receiver was successful and that agreement to the CIDR observation was excellent.

6.   Summary and Concluding Remarks

GNU Radio and USRP, an open-source software toolkit and open-source hardware for SDR, respectively, were utilized for the development of a digital beacon receiver. Based on the first results, shown in the previous section,

it can be concluded that this simple system worked well and that it is useful for real observations. We name it as "GNU Radio Beacon Receiver (GRBR)". Most of the hardware used for developing the GRBR are off-the-shelf universal units and parts. The antenna was also made with quite inexpensive materials. The total cost of the system may be about 1/10 that of the commercial analog beacon receiver. The success of the TEC estimation is largely dependent on the phase coherent design of both USRP and GNU Radio, which has been beautifully achieved. Recent continuous, unattended operation for more than 1 month shows that the system is also very stable. Detailed design information and the software codes of the system are open, and available at the URL http://www.rish.kyoto-u.ac.jp/digitalbeacon/. More development by other users would be greatly appreciated. Our next step is networking the receivers and studying various aspects of the ionospheric variability.

References

Adams, A. T., R. K. Greenough, R. F. Wallenberg, A. Mendelovicz, and C. Lumjiak, The Quadrifilar Helical Antenna, *IEEE Trans. Antennas Propagation*, **AP-22**, 173–179, 1974.

Aitchison, G. J. and K. Weekes, Some deductions of ionospheric information from the observations of emissions from satellite 1957a2-I, *J. Atmos. Terr. Phys.*, **14**, 236–243, 1959.

Bernhardt, P. A. and C. L. Siefring, New satellite-based systems for ionospheric tomography and scintillation region imaging, *Radio Sci.*, **41**, RS5S23, doi:10.1029/2005RS003360, 2006.

Coker, C., G. S. Bust, R. A. Doe, and T. L. Gaussiran II, High-latitude plasma structure and scintillation, *Radio Sci.*, **39**, RS1S15, doi:10.1029/2002RS002833, 2004.

Davies, K., Recent progress in satellite radiobeacon studies with particular emphasis on the ATS-6 radio beacon experiment, *Space Sci. Rev.*, **25**, 357–430, 1980.

De La Beaujardière, O. and the C/NOFS Science Definition Team, C/NOFS: a mission to forecast scintillations, *J. Atmos. Solar-Terr. Phys.*, **66**, 1573–1591, 2004.

Garriott, O. K., The Determination of Ionospheric Electron Content and Distribution from Satellite Observations Part 1. Theory of the Analysis, *J. Geophys. Res.*, **65**(4), 1139–1150, 1960.

Kilgus, C. C., Resonant Quadrifilar Helix, *IEEE Trans. Antennas Propagation*, **AP-17**, 349–351, 1969.

Leitinger, R., G. Schmidt, and A. Tauriainen, An evaluation method combining the differential Doppler measurements from two stations that enables the calculation of electron content of the ionosphere, *J. Geophys.*, **40**, 201–213, 1975.

Leitinger, R., G. K. Hartmann, F. J. Lohmar, and E. Putz, Electron Content Measurement with Geodetic Doppler Receivers, *Radio Sci.*, **19**(3), 789–797, 1984.

Lion, Y.-A., A. G. Pavelyev, S.-F. Liu, A. A. Pavelyev, N. Yen, C.-Y. Huang, and C.-J. Fong, FORMOSAT-3/COSMIC GPS Radio Occultation Mission: Preliminary Results, *IEEE Trans. Geosci. Remote Sensing* **45**(11), 3813–3826, 2007.

Saito, A., S. Fukao, and S. Miyazaki, High resolution mapping of TEC perturbations with the GSI GPS network over Japan, *Geophys. Res. Lett.*, **25**(16), 3079–3082, 1998.

GNU Radio, http://gnuradio.org/.

The Universal Software Radio Peripheral (USRP), http://www.ettus.com/.

M. Yamamoto (e-mail: yamamoto@rish.kyoto-u.ac.jp)